

Cation-Dependent Nuclearity of the Copper–Azido Moiety: Synthesis, Structure, and Magnetic Study

Sandip Saha,[†] Subratanath Koner,^{*,†} Jean-Pierre Tuchagues,[§] Athanassios K. Boudalis,[§] Ken-Ichi Okamoto,^{||} Surajit Banerjee,[‡] and Dasarath Mal[†]

Departments of Chemistry and Physics, Jadavpur University, Jadavpur, Calcutta 700 032, India, Laboratoire de Chimie de Coordination du CNRS, UPR 8241, 205 Route de Narbonne, 31077 Toulouse, Cedex 04, France, and Department of Chemistry, University of Tsukuba, Tsukuba, Ibaraki 305-8571, Japan

Received January 25, 2005

Mono-, di-, and trinuclear copper–azido moieties have been synthesized by varying the size of the counterions. $[\text{Bu}_4\text{N}]^+$ yielded a $[\text{Cu}_2(\text{N}_3)_6]^{2-}$ copper–azido moiety in $[\text{Bu}_4\text{N}]_2[\text{Cu}_2(\mu_{1,1}\text{-N}_3)_2(\text{N}_3)_4]$, **1**, and $[\text{Pr}_4\text{N}]^+$ yielded a $[\text{Cu}_3(\text{N}_3)_8]^{2-}$ moiety in $\{[\text{Pr}_4\text{N}]_2[\text{Cu}_3(\mu_{1,1}\text{-N}_3)_4(\text{N}_3)_4]\}_n$, **2**, in which symmetry-related $[\text{Cu}_3(\text{N}_3)_8]^{2-}$ moieties are doubly $\mu_{1,1}$ -azido bridged to form unprecedented infinite zigzag chains parallel to the crystallographic *a*-axis. In the case of $[\text{Et}_4\text{N}]^+$, the mononuclear species $[\text{Et}_4\text{N}]_2[\text{Cu}(\text{N}_3)_4]$, **3**, has been formed. All complexes have been characterized structurally by single-crystal X-ray analysis: **1**, $\text{C}_{32}\text{H}_{72}\text{N}_{20}\text{Cu}_2$, triclinic, space group $P\bar{1}$, $a = 10.671(9)$ Å, $b = 12.239(9)$ Å, $c = 10.591(5)$ Å, $\alpha = 110.01(4)^\circ$, $\beta = 93.91(5)^\circ$, $\gamma = 113.28(5)^\circ$, $V = 1160.0(1)$ Å³; **2**, $\text{C}_{24}\text{H}_{56}\text{N}_{26}\text{Cu}_3$, monoclinic, space group $P2_1/n$, $a = 8.811(2)$ Å, $b = 37.266(3)$ Å, $c = 13.796(1)$ Å, $\beta = 107.05(1)^\circ$, $V = 4330.8(10)$ Å³; **3**, $\text{C}_{16}\text{H}_{40}\text{N}_{14}\text{Cu}$, tetragonal, space group $I4/m$, $a = b = 10.487(1)$ Å, $c = 12.084(2)$ Å, $V = 1328.9(3)$ Å³. The variable-temperature magnetic susceptibility measurements showed that although the magnetic interaction in $[\text{Bu}_4\text{N}]_2[\text{Cu}_2(\mu_{1,1}\text{-N}_3)_2(\text{N}_3)_4]$, **1**, is antiferromagnetic ($J = -36$ cm⁻¹), it is ferromagnetic in $\{[\text{Pr}_4\text{N}]_2[\text{Cu}_3(\mu_{1,1}\text{-N}_3)_4(\text{N}_3)_4]\}_n$, **2** ($J = 7$ cm⁻¹). As expected, the $[\text{Et}_4\text{N}]_2[\text{Cu}(\text{N}_3)_4]$ complex, **3**, is paramagnetic.

Introduction

The pseudohalide-containing metal complexes have attracted a lot of attention in recent times because of their importance in diverse fields, encompassing condensed matter physics, materials chemistry, biological chemistry, etc.¹ Among them, azide is the most versatile ligand, and its versatility and efficiency lie in its functionality as a terminal

monodentate and a bridging bi-, tri-, and tetradentate ligand. Because of this unique capability, azide attracts a lot of attention in the design of mono- or multidimensional metal-assembled azido complexes.^{2,3} Having control over the molecular dimensions and geometry of the metal–ligand moiety in the compounds may lead to the control over their magnetic properties.² In fact, remarkable structural variations of azido complexes have resulted in a diversity of magnetic behaviors. In this context, the synthesis of nonserendipitous products is particularly interesting for gaining deeper insight into magneto-structural correlations in molecular systems and for developing new functional molecule-based materials. It has been shown that the magnetic interaction mediated by

* To whom correspondence should be addressed. E-mail: skoner55@hotmail.com.

[†] Department of Chemistry, Jadavpur University.

[§] Laboratoire de Chimie de Coordination du CNRS.

^{||} University of Tsukuba.

[‡] Department of Physics, Jadavpur University.

- (1) (a) Kahn, O. *Comments Condens. Matter Phys.* **1994**, *17*, 39. (b) Thomson, L. K.; Tandon, S. K. *Comments Inorg. Chem.* **1996**, *18*, 125 and references therein. (c) Ray, M. S.; Ghosh, A.; Bhattacharya, R.; Mukhopadhyay, G.; Drew, M. G. B.; Ribas, J. *Dalton Trans.* **2004**, 252. (d) Koner, S.; Saha, S.; Mallah, T.; Okamoto, K.-I. *Inorg. Chem.* **2004**, *43*, 840. (e) Koner, S.; Saha, S.; Okamoto, K.-I.; Tuchagues, J.-P. *Inorg. Chem.* **2003**, *42*, 4668. (f) Bhattacharjee, A.; Miyazaki, Y.; Nakazawa, Y.; Koner, S.; Iijima, S.; Sorai, M. *Physica B* **2001**, *305*, 56. (g) Liu, T.-F.; Fu, D.; Gao, S.; Zhang, Y.-Z.; Sun, H.-L.; Su, G.; Liu, Y.-J. *J. Am. Chem. Soc.* **2003**, *125*, 13976. (h) Solomon, E. I.; Sundaram, U. M.; Machonkin, T. E. *Chem. Rev.* **1996**, *96*, 2563. (i) Tuzcek, F.; Solomon, E. I. *Inorg. Chem.* **1993**, *32*, 2850.

- (2) Ribas, J.; Escuer, A.; Monfort, M.; Vicente, R.; Cortés, R.; Lezama, L.; Rojo, T. *Coord. Chem. Rev.* **1999**, *193–195*, 1027 and references therein.

- (3) (a) Ribas, J.; Monfort, M.; Solans, X.; Drillon, M. *Inorg. Chem.* **1994**, *33*, 742. (b) Serna, Z. E.; Lezama, L.; Urriaga, M. K.; Arriortua, M. I.; Barandika, M. G. B.; Cortés, R.; Rojo, T. *Angew. Chem., Int. Ed.* **2000**, *39*, 344. (c) Halcrow, M. A.; Sun, J.-S.; Huffman, J. C.; Christou, G. *Inorg. Chem.* **1995**, *34*, 4167. (d) Papaefstathiou, G. S.; Perlepes, S. P.; Escuer, A.; Vicente, R.; Font-Barida, M.; Solans, X. *Angew. Chem., Int. Ed.* **2001**, *40*, 884.

the azido bridge is generally antiferromagnetic for the $\mu_{1,3}$ -N₃ (end-to-end, EE) mode, though, in the recent past, some exceptions have been reported.⁴ For the $\mu_{1,1}$ -N₃ (end-on, EO) bridging mode, ferromagnetic ordering is established when the Cu–N–Cu angle is small, which has been attributed to a spin-polarization effect.⁵ However, J_{ferro} is expected to decrease with increasing Cu–N–Cu angle, and the EO azido bridge can propagate antiferromagnetic coupling if the bridge angle is large enough (critical angle $\sim 108^\circ$).^{5,6} More recent theoretical studies suggest a smaller critical angle ($\sim 104^\circ$).⁷ Other structural parameters, such as Cu–N (azido) distance, mean out-of-plane deviation of the azido group, geometry of the ligand environment to the Cu^{II} centers, etc., shall also be considered.^{6,7} Therefore, EO azido-bridged polynuclear metal complexes certainly have relevance to the field of molecular magnetism. Different types of polymeric structures, 1D [Cu₂($\mu_{1,1}$ -N₃)₄(3-picoline)₂]_n,⁸ [Cu₃($\mu_{1,1}$ -N₃)₅($\mu_{1,1,1}$ -N₃)(2-benzoylpy)₂]_n,⁹ [Cu($\mu_{1,1}$ -N₃)₂(3,4-lutidine)]_n,¹⁰ [Cu₃($\mu_{1,1}$ -N₃)₆(2,6-lutidine)₂]_n,¹⁰ [Cu($\mu_{1,1}$ -N₃)₂(py-N-oxide)]_n,¹¹ [Cu($\mu_{1,1}$ -N₃)₂(2-Me,5-Etpy)]_n,¹² [Cu($\mu_{1,1}$ -N₃)₂(2-Clpy)]_n,¹³ [Cu($\mu_{1,3}$ -N₃)₂(3-benzoylpy)]_n,¹³ {[Cu($\mu_{1,1}$ -N₃)($\mu_{1,1,3}$ -N₃)(3-Etpy)₂][Cu($\mu_{1,3}$ -N₃)₂(3-Etpy)₂]}_n,¹⁴ {[Cu₂($\mu_{1,1}$ -N₃)₄(3-Clpy)₄][Cu($\mu_{1,3}$ -N₃)₂(3-Clpy)₂]}_n,¹⁵ and [Cu₂($\mu_{1,1}$ -N₃)₂($\mu_{1,1,1}$ -N₃)($\mu_{1,1,3}$ -N₃)(2-bis(pyrazol-1-yl)methane)]_n¹⁶ and 2D [Cu($\mu_{1,1}$ -N₃)₂(2,3-diMepy)]_n¹² and [Cu($\mu_{1,1}$ -N₃)($\mu_{1,3}$ -N₃)(4-Etpy)₂]_n,¹⁴ were found for several copper–azido systems including ancillary ligands. To our knowledge, the only polymeric (1D) copper–azido system devoid of ancillary ligands is {[Me₄N]-[Cu(N₃)₃]}_n, in which the copper(II) cations are connected by a triple bridge including two $\mu_{1,3}$ -N₃ and one $\mu_{1,1}$ -N₃ bridging anions.¹⁷ On the other hand, a diversity of structural and magnetic behaviors has been observed among Mn^{II}–azido moieties simply by varying the size of the

countercations. A small positive counterion, Cs⁺, afforded an interesting 3D-stacked honeycomb Cs_n{[Mn(N₃)₃]}_n where Cs⁺ ions were entrapped in the hole of the 3D metal–azido network; this is also the case for a cation such as [Me₄N]⁺.^{17–19} But, for a bigger cation, tetraethylammonium, a polymeric double-chain type structure was found in the complex [Et₄N]_n[Mn₂(N₃)₅(H₂O)_n].¹⁸ The magnetic properties of copper–azido polymeric structures have seldom been reported. A weak ferromagnetic interaction (6.2 cm⁻¹, $-2J_1S_1S_2$ formalism) has been evaluated in [Cu($\mu_{1,1}$ -N₃)($\mu_{1,3}$ -N₃)(4-Etpy)₂]_n¹⁴ by neglecting the weak antiferromagnetic interaction that may be expected through the EE azido bridges and by considering EO azido-bridged dinuclear units as an approximation. A combination of alternating $-J_1J_1-J_2J_2$ -ferromagnetic (5.3 cm⁻¹) and antiferromagnetic (-9.8 cm⁻¹) interactions within a ring of 12 local $S = 1/2$ centers (analytical expression) has been considered as an approximation for evaluating the magnetic behavior of {[Cu₂($\mu_{1,1}$ -N₃)₄(3-Clpy)₄][Cu($\mu_{1,3}$ -N₃)₂(3-Clpy)₂]}_n.¹⁵ A weak ferromagnetic interaction has been evaluated in [Cu₂($\mu_{1,1}$ -N₃)₂($\mu_{1,1,1}$ -N₃)($\mu_{1,1,3}$ -N₃)(2-bis(pyrazol-1-yl)methane)]_n¹⁶ by neglecting the very weak antiferromagnetic interaction that may be expected through the intertetranuclear EE azido bridges, by approximating the interactions through the long EO azido bridges with a molecular-field correction term, θ (-0.4 K), and by considering the short EO azido bridges as the main magnetic mediators yielding intradinuclear ferromagnetic interactions (5.9 cm⁻¹, $-2J_1S_1S_2$ formalism). Finally, a weak antiferromagnetic interaction ($J/k = -3.6$ K) has been evaluated in {[Me₄N][Cu(N₃)₃]}_n by considering interactions between nearest neighbors of a Heisenberg chain, with the thermal variation of the magnetic susceptibility being approximated by an empirical function.¹⁷

Further exploration of copper(II)–azido systems based on various countercations has allowed us to structurally and magnetically characterize Cu^{II}–azido systems containing either tetraethylammonium, tetrapropylammonium, or tetrabutylammonium countercations. Interestingly, the variation in the size of the cations yielded diverse copper(II)–azido nuclearities as well as magnetic properties: [Bu₄N]₂[Cu₂($\mu_{1,1}$ -N₃)₂(N₃)₄], **1**, is dinuclear and shows an antiferromagnetic behavior; {[Pr₄N]₂[Cu₃($\mu_{1,1}$ -N₃)₄(N₃)₄]}_n, **2**, consists of bis- $\mu_{1,1}$ -N₃-bridged linear trinuclear copper(II)–azido moieties and shows a ferromagnetic behavior; [Et₄N]₂[Cu(N₃)₄], **3**, is mononuclear and shows a paramagnetic behavior. It is noteworthy that none of these complexes have any coligands.

Experimental Section

Materials. Copper(II) nitrate trihydrate (Aldrich) and sodium azide (Sigma) were used without further purification. All other chemicals used were of AR grade.

Synthesis. Caution! Although our samples never exploded during handling, azide metal complexes are potentially explosive: only a small amount of material should be prepared, and it should be handled with care.

- (4) (a) Maji, T. K.; Mukherjee, P. S.; Mostafa, G.; Mallah, T.; Cano-Boquera, J.; Chaudhuri, N. R. *Chem. Commun.* **2001**, 1012. (b) Shen, Z.; Zuo, J.-L.; Gao, S.; Song, Y.; Che, C.-M.; Fun, H.-K.; You, X.-Z. *Angew. Chem., Int. Ed.* **2000**, *39*, 3633. (c) Hong, C. S.; Koo, J.; Son, S.-K.; Lee, Y. S.; Kim, Y.-S.; Do, Y. *Chem.–Eur. J.* **2001**, *7*, 4243.
- (5) (a) Sikorav, S.; Bkouche-Waksman, I.; Kahn, O. *Inorg. Chem.* **1984**, *23*, 490. (b) Kahn, O.; Mallah, T.; Gouteron, J.; Jeannin, S.; Jeannin, Y. *J. Chem. Soc., Dalton Trans.* **1989**, 1117.
- (6) (a) Cortes, R.; Urtiaga, R. K.; Lezama, L.; Larramendi, J. R.; Arriortua, M. I.; Rojo, T. *J. Chem. Soc., Dalton Trans.* **1993**, 3685. (b) Tandon, S. S.; Thompson, L. K.; Manuel, M. E.; Bridson, J. N. *Inorg. Chem.* **1994**, *33*, 5555. (c) Thompson, L. K.; Tandon, S. S.; Manuel, M. E. *Inorg. Chem.* **1995**, *34*, 2356.
- (7) (a) Aebbersold, M. A.; Gillon, B.; Plantevin, O.; Pardi, L.; Kahn, O.; Bergerat, P.; von Seggern, I.; Tuzek, F.; Öhrström, L.; Grand, A.; Lelièvre-Berna, E. *J. Am. Chem. Soc.* **1998**, *120*, 5238. (b) Ruiz, E.; Cano, J.; Alvarez, S.; Alemany, P. *J. Am. Chem. Soc.* **1998**, *120*, 11122. (c) Adamo, C.; Barone, V.; Bencini, A.; Totti, F.; Ciofini, I. *Inorg. Chem.* **1999**, *38*, 1996.
- (8) Goher, M. A. S.; Mak, T. C. W. *Inorg. Chim. Acta* **1984**, *89*, 119.
- (9) Goher, M. A. S.; Mak, T. C. W. *Inorg. Chim. Acta* **1985**, *99*, 223.
- (10) Mautner, F. A.; Goher, M. A. S. *Polyhedron* **1994**, *13*, 2141.
- (11) Goher, M. A. S.; Mautner, F. A. *Polyhedron* **1995**, *14*, 1751.
- (12) Goher, M. A. S.; Al-Salem, N. A.; Mautner, F. A. *Polyhedron* **1996**, *15*, 4513.
- (13) Goher, M. A. S.; Mautner, F. A. *Polyhedron* **1998**, *17*, 1561.
- (14) Goher, M. A. S.; Escuer, A.; Abu-Youssef, M. A. M.; Mautner, F. A. *Polyhedron* **1998**, *17*, 4265.
- (15) Escuer, A.; Vicente, R.; El Fallah, M. S.; Goher, M. A. S.; Mautner, F. A. *Inorg. Chem.* **1998**, *37*, 4466.
- (16) Zhang, L.; Tang, L.-F.; Wang, Z.-H.; Du, M.; Julve, M.; Lloret, F.; Wang, J.-T. *Inorg. Chem.* **2001**, *40*, 3619.
- (17) Mautner, F. A.; Hanna, S.; Cortés, R.; Lezama, L.; Barandika, M. G.; Rojo, T. *Inorg. Chem.* **1999**, *38*, 4647.

- (18) Goher, M. A. S.; Cano, J.; Journaux, Y.; Abu-Youssef, M. A. M.; Mautner, F. A.; Escuer, A.; Vicente, R. *Chem.–Eur. J.* **2000**, *6*, 778.
- (19) Mautner, F. A.; Cortés, R.; Lezama, L.; Rojo, T. *Angew. Chem., Int. Ed. Engl.* **1996**, *35*, 78.

Synthesis of Compounds 1, 2, and 3. All three compounds were prepared by following a similar process. A methanolic solution (15 mL) containing copper(II) nitrate trihydrate (0.25 g, 1.03 mmol) was mixed with an aqueous solution of sodium azide (0.75 g, 11.54 mmol) dissolved in a minimum volume of water. An aqueous solution of either tetrabutyl- (1), tetrapropyl- (2), or tetraethylammonium bromide (3) (0.94 mmol) was added to this reaction mixture with continuous stirring. The stirring was continued for another 2 h, and a black precipitate was obtained. It was then filtered off and dried in a desiccator. Black block crystals of compounds 1, 2, and 3 suitable for X-ray analysis were obtained upon slow evaporation of the dark mother liquor at room temperature. $[\text{Bu}_4\text{N}]_2[\text{Cu}_2(\mu_{1,1}\text{-N}_3)_2(\text{N}_3)_4]$, **1**, was obtained in ca. 90% yield. Anal. Calcd for $\text{C}_{32}\text{H}_{72}\text{N}_{20}\text{Cu}_2$: C, 44.5; H, 8.4; N, 32.4%. Found: C, 44.5; H, 7.8; N, 32.8%. IR (KBr pellets, cm^{-1}): ν_{as} (azido) 2070, 2039. $[\text{Pr}_4\text{N}]_2[\text{Cu}_3(\mu_{1,1}\text{-N}_3)_4(\text{N}_3)_4]$, **2**, was obtained in ca. 70% yield. Anal. Calcd for $\text{C}_{24}\text{H}_{56}\text{N}_{26}\text{Cu}_3$: C, 32.2; H, 6.3; N, 40.7%. Found: C, 32.2; H, 6.0; N, 41.4%. IR (KBr pellets, cm^{-1}): ν_{as} (azido) 2140, 2040. $[\text{Et}_4\text{N}]_2[\text{Cu}(\text{N}_3)_4]$, **3**, was obtained in ca. 20% yield. Anal. Calcd for $\text{C}_{16}\text{H}_{40}\text{N}_{14}\text{Cu}$: C, 39.0; H, 8.2; N, 39.8%. Found: C, 38.8; H, 8.4; N, 40.1%. IR (KBr pellets, cm^{-1}): ν_{as} (azido) 2040. Though the X-ray quality single crystals of complex **1** were obtained within 2–3 days, it took several weeks to obtain single crystals of **2** and **3** that were suitable for X-ray analysis.

Physical Measurements. The facilities used for all physical measurements and the specific procedure used for fitting the magnetic data have been described previously.^{1e}

X-ray Crystallography. A black plate crystal of **1** was selected for collecting X-ray data on a Rigaku AFC7S diffractometer with graphite-monochromated Mo K α radiation ($\lambda = 0.71073 \text{ \AA}$). Over the course of data collection, the standards decreased by 4.2%. The structure was solved by direct methods (SIR 92)²⁰ and expanded using Fourier techniques.²¹ The structure was refined by full-matrix least-squares on F^2 using anisotropic thermal parameters for non-hydrogen atoms. The hydrogen atoms were included but not refined. Atomic scattering factors were taken from ref 22. All calculations were performed using the TeXsan crystallographic software package of Molecular Structure Corp.²³ The max and min peaks on the final difference Fourier map were 0.83 and $-1.08 \text{ e}^- \text{ \AA}^{-3}$, respectively. Crystallographic data for complex **1** are summarized in Table 1. Bruker P4 and Bruker-Nonius CAD4 diffractometers with graphite-monochromated Mo K α radiation ($\lambda = 0.7093 \text{ \AA}$) and $\omega-2\theta$ scan mode were used to collect X-ray data from rectangular block crystals of complexes **2** and **3**, respectively. Over the course of data collection, the standards decreased by 3%. The structures of **2** and **3** were solved and refined with SHELXS 97 and SHELXL 97, respectively.²⁴ The structures were refined by full-matrix least-squares on F^2 using anisotropic thermal parameters for non-hydrogen atoms. The hydrogen atoms were included but not refined. The max and min peaks on the final difference Fourier map were 0.435 and $0.371 \text{ e}^- \text{ \AA}^{-3}$ and -0.556 and $-0.215 \text{ e}^- \text{ \AA}^{-3}$ for **2** and

Table 1. Summary of Crystal Data and Refinement Parameters for Complexes 1–3

	1	2	3
formula	$\text{C}_{32}\text{H}_{72}\text{N}_{20}\text{Cu}_2$	$\text{C}_{24}\text{H}_{56}\text{N}_{26}\text{Cu}_3$	$\text{C}_{16}\text{H}_{40}\text{N}_{14}\text{Cu}$
<i>a</i> (Å)	10.671(9)	8.811(2)	10.487(1)
<i>b</i> (Å)	12.239(9)	37.266(3)	10.487(1)
<i>c</i> (Å)	10.591(5)	13.796(1)	12.084(2)
α (deg)	110.01(4)	90.0	90.0
β (deg)	93.91(5)	107.05(1)	90.0
γ (deg)	113.28(5)	90.0	90.0
<i>V</i> (Å ³)	1160.0(1)	4330.8(10)	1328.9(3)
<i>Z</i>	1	4	2
space group	$P\bar{1}$	$P2_1/n$	$I4/m$
ρ_{calc} (g cm ⁻³)	1.237	1.446	1.212
<i>F</i> (000)	462	1876	526
μ (Mo K α) (mm ⁻¹)	0.962	1.511	0.852
R1, wR2	0.063, 0.167	0.0457, 0.1028	0.0343, 0.1095
GOF (<i>S</i>)	1.070	1.060	1.211
unique reflns	5326	5692	1470
observed reflns	1664	4182	767
[<i>I</i> > 2 σ (<i>I</i>)]			
max Δ /esd	1.048	0.000	0.000
final $\Delta\rho$, max/min (e Å ⁻³)	0.83, -1.08	0.435, -0.556	0.371, -0.215

3, respectively. Crystallographic data for complexes **2** and **3** are also summarized in Table 1.

Results and Discussion

X-ray Structure of Complexes 1, 2, and 3. The structure of **1** consists of $[\text{Cu}_2(\text{N}_3)_6]_2^{2-}$ anions (Figure 1) and tetrabu-

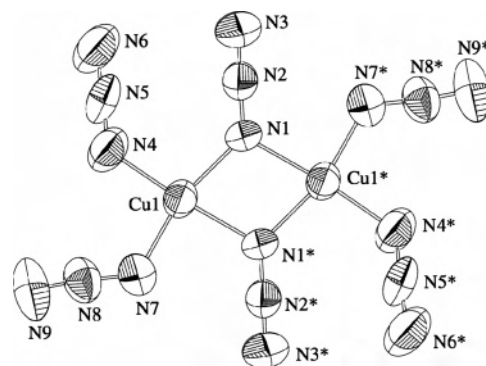


Figure 1. ORTEP view of the $[\text{Cu}_2(\mu_{1,1}\text{-N}_3)_2(\text{N}_3)_4]^{2-}$ anion of complex **1** with an atom numbering scheme.

tylammonium cations. Selected bond lengths and bond angles are collected in Table 2. The two symmetry-related ($-x, -y, -z$) copper centers of the dinuclear complex anion are coordinated by four nitrogen atoms: two from terminal azido groups with Cu–N distances of 1.906(5) and 1.912(5) Å and two from EO pseudosymmetrically bridging azido ligands with Cu–N distances of 1.953(5) and 2.006(4) Å. The Cu1–N1–Cu1* (=Cu1*–N1*–Cu) angle is 104.3(2)°. The coordination environment around each copper cation may be described as distorted square planar. The Cu–Cu separation within the dinuclear complex anion is 3.126(2) Å, similar to that of the other reported cases.²⁵ **1** is the first example of a Cu^{II} compound including exclusively azido ligands acting

- (20) Altmire, A.; Cascarano, G.; Giovazzo, C.; Gugaliradi, A.; Burla, M. C.; Polidori, G.; Camalli, M. *J. Appl. Crystallogr.* **1994**, *27*, 435.
 (21) Beurskens, P. T.; Admiraal, G.; Beurskens, G.; Bosman, W. P.; de Gelder, R.; Israel, R.; Smits, J. M. M. *DIREX 94: The DIRDIF 94 program system, Technical Report of the Crystallography Laboratory*; University of Nijmegen: The Netherlands, 1994.
 (22) Cromer, D. T.; Waber, J. T. *International Tables for X-ray Crystallography*; The Kynoch Press: Birmingham, England, 1974; Vol. IV, Table 2.2 A.
 (23) *TeXsan: Crystal Structure Analysis Package*; Molecular Structure Corp., 1985 and 1999.
 (24) Sheldrick, G. M. *SHELX 97: Package for Crystal Structure Solution and Refinement*; University of Göttingen: Göttingen, Germany, 1997.

- (25) (a) Tandon, S. S.; Thompson, L. K.; Bridson, J. N.; McKee, V.; Downard, A. J. *Inorg. Chem.* **1992**, *31*, 4635. (b) Goher, M. A. S.; Al-Salem, N. A.; Mautner, F. A.; Klepp, K. O. *Polyhedron* **1997**, *16*, 825. (c) Escuer, A.; Goher, M. A. S.; Mautner, F. A.; Vicente, R. *Inorg. Chem.* **2000**, *39*, 2107.

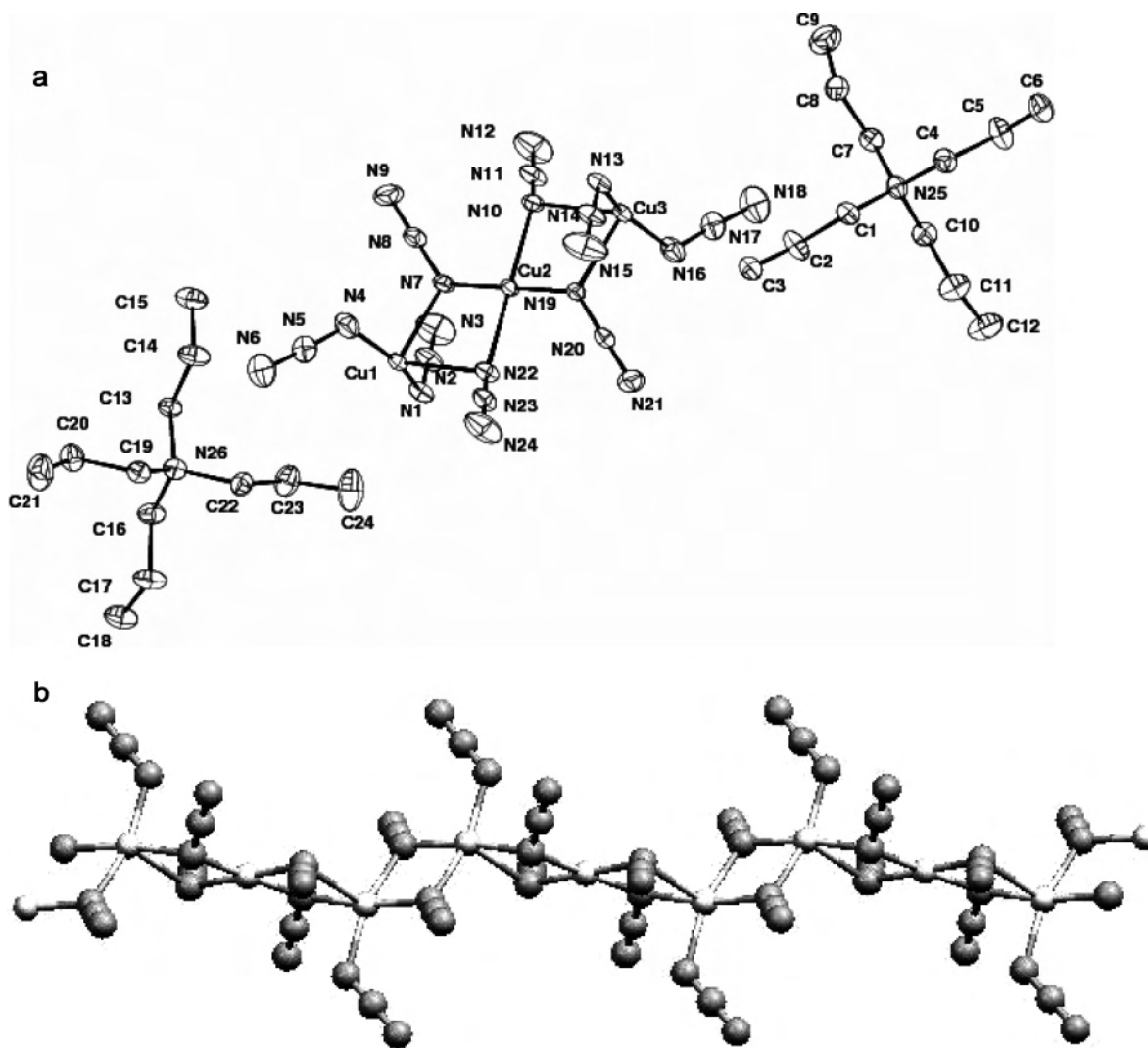


Figure 2. (a) ORTEP view of complex **2**, $[\text{Pr}_4\text{N}]_2[\text{Cu}_3(\mu_{1,1}\text{-N}_3)_4(\text{N}_3)_4]$, with an atom numbering scheme. (b) A zigzag 1D chain of $[\text{Cu}_3(\mu_{1,1}\text{-N}_3)_4(\text{N}_3)_4]^{2-}$ complex anions.

either as terminal donors or as $\mu_{1,1}\text{-N}_{\text{azido}}$ bridges. Its structure is related to, but is different from, that of the $[\text{Cu}_2(\text{N}_3)_6]^{2-}$ complex anion of the $\{[\text{Cu}_2(\text{tppz})(\text{N}_3)_2][\text{Cu}_2(\text{N}_3)_6]\}_n$ polymer, where one copper is pentacoordinated and two terminal azido ligands also act as $\mu_{1,1}\text{-N}_{\text{azido}}$ bridges.²⁶

The crystallographic asymmetric unit of complex **2** consists of a trinuclear $[\text{Cu}_3(\mu_{1,1}\text{-N}_3)_4(\text{N}_3)_4]^{2-}$ anion and two tetrapropylammonium cations. A perspective view of the asymmetric unit with an atom numbering scheme is given in Figure 2a, and selected bond lengths and angles are listed in Table 2. The copper centers are exclusively coordinated by azido nitrogen atoms, and they are bridged in an EO mode only. The two halves of the complex anion are related by a pseudocenter of inversion located at the central copper cation, Cu2. The tetrapropylammonium cations, however, are not related by this pseudoinversion center. The coordination environment of the central Cu2 cation can be better described as distorted square planar with a maximum deviation of any in-plane atom from the least-squares plane through Cu2, N7,

N10, N19, and N22 of 0.012(5) Å. The Cu1 and Cu3 copper(II) centers, coordinated by four bridging and one terminal azido ligands, display a distorted square pyramidal geometry. While N1, N4, N7, and N13' (N1', N13, N19, and N16) occupy the basal positions of the bipyramidal coordination environment of Cu1 (Cu3), the apical position is occupied by N22 (N10). The trigonality index ($\tau = (\phi_1 - \phi_2)/60$, where ϕ_1 and ϕ_2 are the two largest L–M–L angles of the coordination sphere)²⁷ has been calculated for the two pentagonal copper sites. $\tau = 0.209$ and 0.206 for Cu1 and Cu3, respectively, confirming the square pyramidal character of both sites ($\tau = 0$ infers a perfect square pyramid, and $\tau = 1$ infers a perfect trigonal bipyramid). The pentacoordinated Cu1 and Cu3 cations are pseudosymmetrically bridged to the symmetry-related ($-x, -y, -z$) Cu3 and Cu1 cations of neighboring trinuclear units through the above-mentioned pairs of EO azido ligands (N1 and N13' and N13 and N1', respectively) to form a zigzag 1D chain (Figure 2b). **2** is the

(26) Carranza, J.; Brennan, C.; Sletten, J.; Clemente-Juan, J. M.; Lloret, F.; Julve, M. *Inorg. Chem.* **2003**, *42*, 8716.

(27) (a) Hathaway, B. J. *Struct. Bonding* **1973**, *14*, 49. (b) Addison, A. W.; Nageswara, T.; Reedijk, J.; van Rijn, J.; Verchoor, G. C. *J. Chem. Soc., Dalton Trans.* **1984**, 1349.

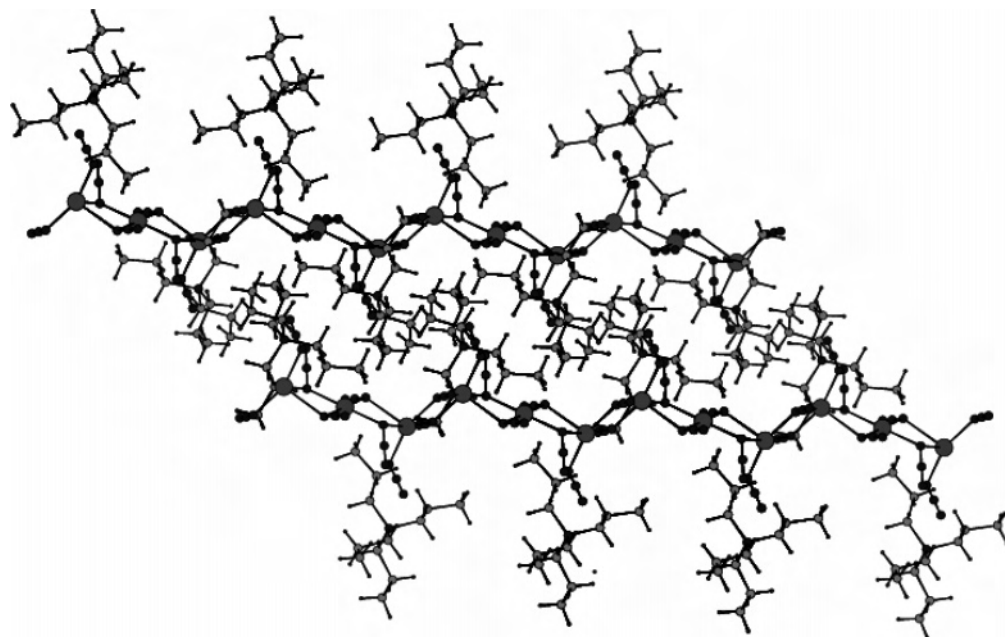


Figure 3. Perspective view showing two chains of $[\text{Cu}_3(\mu_{1,1}\text{-N}_3)_4(\text{N}_3)_4]^{2-}$ complex anions together with the intercalated $[\text{Pr}_4\text{N}]^+$ cations.

first example of a Cu^{II} 1D chain including exclusively azido ligands acting either as terminal donors or as $\mu_{1,1}\text{-N}_{\text{azido}}$ bridges. Its structure is significantly different from that of $\{[\text{Me}_4\text{N}][\text{Cu}(\text{N}_3)_3]\}_n$, where the Cu^{II} cations are connected by a triple bridge including two $\mu_{1,3}\text{-N}_3$ anions and one $\mu_{1,1}\text{-N}_3$ anion.¹⁷ The tetrapropylammonium cations occupy the void space between the $\{[\text{Cu}_3(\mu_{1,1}\text{-N}_3)_6(\text{N}_3)_2]^{2-}\}_n$ chains. The $\text{Cu}1\cdots\text{Cu}2$ and $\text{Cu}2\cdots\text{Cu}3$ distances in the complex anion are 3.178 and 3.176 Å, respectively, whereas $\text{Cu}1\cdots\text{Cu}3'$ ($\text{Cu}3\cdots\text{Cu}1'$) = 3.105 Å. The $\text{Cu}1\text{-N}1\text{-Cu}3'$ ($\text{Cu}1\text{-N}1'\text{-Cu}3'$) and $\text{Cu}3\text{-N}13\text{-Cu}1'$ ($\text{Cu}1\text{-N}13'\text{-Cu}3'$) angles are equal to 101.02° and 102.13°, respectively. Other distances and angles are in the range of the corresponding reported data.^{8–17} The azido ligands with $(\text{Cu}\text{-})\text{N}\text{-N}$ distances of 1.176(7)–1.227(8) Å and $(\text{Cu}\text{-})\text{N}\text{-N}$ distances of 1.128(6)–1.159(7) Å and $\text{N}\text{-N}\text{-N}$ bond angles of 176.1(8)–179.7(7)° are almost linear. The bulky tetrapropylammonium cations are of expected geometry and provide an interchain distance of ~ 10.5 Å and numerous hydrogen contacts between anions and cations. The nitrogen atoms of two terminal (N6, N18) and three bridging azido ligands (N9, N21, N24) are hydrogen bonded to the carbon atoms of the $[\text{Pr}_4\text{N}]^+$ cations. The C1 and C11 atoms of the $[\text{Pr}_4\text{N}]^+$ cations are connected by two bridging azido ligands (N21, N24) related by inversion and translation along the [101] direction. Other hydrogen contacts between translation-related anions and cations result in a complex network of hydrogen bonds in complex 2.

The crystal structure of complex 3 consists of discrete monomeric $[\text{Cu}(\text{N}_3)_4]$ anions and tetraethylammonium cations (Figure 4), and selected bond lengths and angles are given in Table 2. The copper(II) center lying on the 4/m site (0, 0, 0) is surrounded by four symmetry-related azido ligands, forming a square planar CuN_4 arrangement. The coordinated azido anions are nearly linear, but the $(\text{Cu}\text{-})\text{N}\text{-N}$ bond length (1.185(3) Å) is longer than the

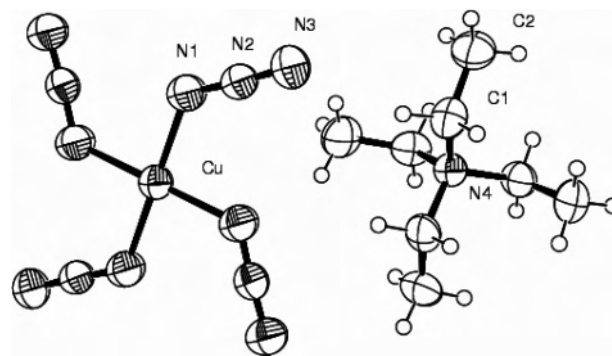


Figure 4. ORTEP view of complex 3, $[\text{Et}_4\text{N}]_2[\text{Cu}(\text{N}_3)_4]$, with an atom numbering scheme.

($\text{Cu}\text{-N}\text{-})\text{N}\text{-N}$ bond distance (1.142(3) Å). This result suggests that the covalency of the $\text{Cu}^{\text{II}}\text{-azido}$ bond is appreciable, and the main contribution to the ground-state geometry of the coordinated azido is provided by the two canonical structures, $\text{-N}=\text{N}^+=\text{N}^- \leftrightarrow \text{-N}^-\text{-N}^+\equiv\text{N}$.

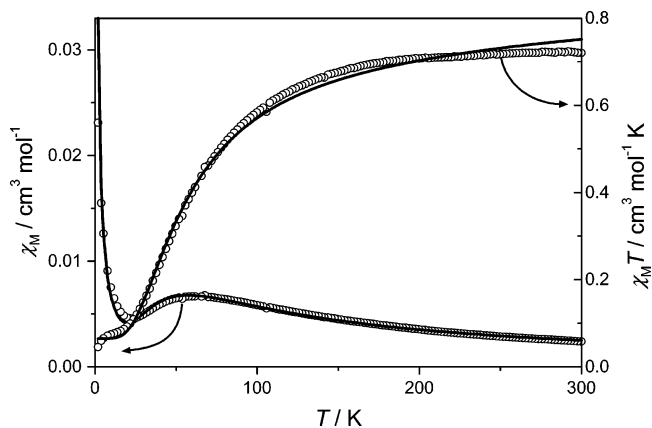
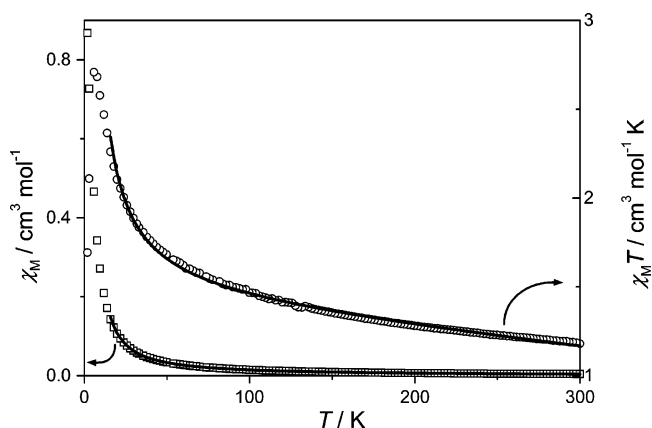
Magnetic Properties. The temperature dependence of the molar magnetic susceptibility, χ_M , for complexes 1, 2, and 3 in the 2–300 K temperature range was measured with a Quantum Design MPMS superconducting quantum interference device (SQUID) magnetometer under magnetic fields of 20 kG (for 1) and 10 kG (for 2 and 3) and is shown in Figures 5 and 6 for 1 and 2, respectively. The $\chi_M T$ value of 0.72 $\text{cm}^3\cdot\text{mol}^{-1}\cdot\text{K}$ at 300 K for complex 1 is slightly smaller than the value expected for two magnetically uncoupled copper(II) ions ($\chi_M T = 0.75 \text{ cm}^3\cdot\text{mol}^{-1}\cdot\text{K}$ for $g = 2.0$), whereas the $\chi_M T$ value is 1.18 $\text{cm}^3\cdot\text{mol}^{-1}\cdot\text{K}$ at 300 K for complex 2, which is slightly higher than the value expected for three magnetically uncoupled copper(II) ions ($\chi_M T = 1.12 \text{ cm}^3\cdot\text{mol}^{-1}\cdot\text{K}$ for $g = 2.0$). Upon cooling, the $\chi_M T$ value for complex 1 decreases gradually with temperature until ca. 175 K and then decreases rapidly, reaching a minimum of 0.045 $\text{cm}^3\cdot\text{mol}^{-1}\cdot\text{K}$ at 1.96 K, indicating a bulk antiferromagnetic

Table 2. Selected Bond Distances (Å) and Bond Angles (deg) of Complexes 1–3

Complex 1			
Cu1–N1	1.953(5)	Cu1–N1*	2.006(4)
Cu1–N7	1.912(5)	Cu1–N4	1.906(5)
N2–N3	1.139(6)	N1–N2	1.208(5)
N5–N6	1.163(7)	N4–N5	1.164(6)
N8–N9	1.129(6)	N7–N8	1.198(6)
N10–C5	1.511(6)	N10–C1	1.527(5)
N10–C13	1.526(6)	N10–C9	1.510(6)
Cu1–N1–Cu1*	104.3(2)	N1–Cu1–N7	163.9(2)
N1–Cu1–N4	100.0(2)	N1–Cu1–N1*	75.7(2)
N4–Cu1–N7	95.0(2)	N7–Cu1–N1*	89.7(2)
N4–Cu1–N1*	173.7(2)	N1–N2–N3	178.4(6)
Complex 2			
Cu1–N1	2.032(5)	Cu1–N4	1.946(5)
Cu1–N7	2.029(4)	Cu1–N22	2.348(4)
Cu1–N13'	1.990(4)	Cu2–N7	2.002(4)
Cu2–N10	1.961(4)	Cu2–N19	2.001(4)
Cu2–N22	1.957(4)	Cu3–N10	2.334(5)
Cu3–N13	2.002(4)	Cu3–N16	1.944(5)
Cu3–N19	2.041(4)	Cu3–N1'	1.992(4)
N1–Cu1–N4	157.8(2)	N1–Cu1–N7	92.9(2)
N1–Cu1–N22	104.8(2)	N4–Cu1–N7	90.4(2)
N4–Cu1–N22	97.2(2)	N7–Cu1–N22	74.5(2)
N7–Cu2–N10	95.6(2)	N7–Cu2–N19	179.3(2)
N7–Cu2–N22	84.5(2)	N10–Cu2–N19	84.4(2)
N10–Cu2–N22	179.9(2)	N19–Cu2–N22	95.5(2)
N10–Cu3–N13	103.8(2)	N10–Cu3–N19	74.6(2)
N10–Cu3–N16	97.8(2)	N13–Cu3–N16	158.2(2)
N13–Cu3–N19	92.3(2)	N16–Cu3–N19	90.7(2)
Cu2–N7–Cu1	104.0(2)	Cu2–N10–Cu3	94.98(18)
Cu2–N22–Cu1	94.68(18)	Cu2–N19–Cu3	103.6(2)
Cu1–N1–Cu3'	101.0(2)	Cu3–N13–Cu1'	102.1(3)
Cu1–N1'–Cu3'	101.0(2)	Cu1–N13'–Cu3'	102.1(3)
Complex 3			
Cu–N1	1.975(2)	N1–N2	1.185(3)
N2–N3	1.142(3)	N4–C1	1.521(2)
C1–C2	1.506(3)	N(1)#1–Cu–N(1)	180.00(14)
N(1)–Cu–N(1)#2	90.0	N(1)#1–Cu–N(2)#2	90.0
N(3)–N(2)–N(1)	176.4(3)		

behavior. On the other hand, for complex **2**, upon cooling, $\chi_M T$ increases gradually until ca. 75 K and then increases rapidly, reaching a maximum of $2.71 \text{ cm}^3 \cdot \text{mol}^{-1} \cdot \text{K}$ at 5.8 K, indicating the operation of a dominant ferromagnetic interaction between the copper centers of complex **2**. A slight decrease of $\chi_M T$ below 5.8 K will be discussed later. The $\chi_M T$ value for complex **3** is equal to $0.36 \pm 0.02 \text{ cm}^3 \cdot \text{mol}^{-1} \cdot \text{K}$ over the whole temperature range, confirming the paramagnetic nature of this mononuclear species.

To model the magnetic properties of complex **1**, a simple isotropic model of two magnetically coupled $S = 1/2$ spins was considered ($H = -2J\hat{S}_1 \cdot \hat{S}_2$, spin Hamiltonian). Fitting of the data, with the g factor set to 2 and considering a paramagnetic impurity fraction ρ , yielded the parameter values of $J = -36(2) \text{ cm}^{-1}$ and $\rho = 4.3\%$ with an agreement factor of $R = 2.7 \times 10^{-3}$. Figure 5 shows the result of this fit. A comparison with the few reported complexes containing the symmetrical or pseudosymmetrical $[\text{Cu}_2(\text{N}_3)_6]$ core (Table 3)^{25,26} confirms that among the magnetostructural correlations considered in the literature (see Introduction), i.e., J vs the Cu–N–Cu θ -angle, θ is the prevailing factor. Indeed, among the complexes collated in Table 3, only those ($[\text{Cu}_2(\text{H}_2\text{L}_2)]$ $[\text{Cu}_2(\text{N}_3)_6]$ ^{25a} and **1**) having the larger θ -angle ($\sim 104^\circ$) exhibit antiferromagnetic interactions, whereas among those having a smaller θ -angle (102.5 –

**Figure 5.** χ_M vs T and $\chi_M T$ vs T experimental data for complex **1**. The solid lines result from a least-squares fit of the data with the model described in the text.**Figure 6.** χ_M vs T and $\chi_M T$ vs T experimental data for complex **2**. The solid lines result from a least-squares fit of the data with the model described in the text.

103°), $\{[\text{Cu}_2(\text{tppz})(\text{N}_3)_2][\text{Cu}_2(\text{N}_3)_6]\}_n$ ²⁶ exhibits weak ferromagnetic interactions; magnetic properties have not been reported for $\{\text{K}_2[\text{Cu}_2(\text{N}_3)_6][\text{Cu}(\text{pyrazinato})(\text{N}_3)]\}_n$.^{25b} Interestingly, these results agree with the lower value ($\sim 104^\circ$) recently predicted for the critical angle.⁷ As shown by Table 3, regardless of their ferro- or antiferromagnetic behavior, the four compounds have similar Cu–N and Cu...Cu distances, confirming the conclusions drawn by Escuer et al.^{25c}

Although the structural analysis of complex **2** shows that there is no symmetry operation within the trimetallic repeat unit, the pairs of Cu1–N_{azido}–Cu2 and Cu2–N_{azido}–Cu3 angles are very similar (Cu1–N7–Cu2 = 104.02° , Cu1–N22–Cu2 = 94.67° , Cu2–N10–Cu3 = 95.00° , and Cu2–N19–Cu3 = 103.55°), allowing us to consider a single exchange constant, J , for both interactions despite the absence of an inversion center. A rigorous analysis would require a different exchange constant, J' , for the intertrimer interaction characterized by the Cu1–N1–Cu3' and Cu3–N13–Cu1' angles of 101.02° and 102.13° , respectively. However, considering that the average values for Cu1–N_{azido}–Cu2, Cu2–N_{azido}–Cu3, and Cu3–N_{azido}–Cu1' are close to each other, this could lead to overparametrization, and furthermore, it would make the problem intractable because there is no analytical expression for a ferromagnetic J – $J \cdots J'$ – $J \cdots J$ chain.

Table 3. Comparison of Metric Parameters and Magnetic Interactions for Complexes Containing the [Cu₂(N₃)₆] Core

compound	Cu–N1 (Å)	Cu–N1* (Å)	Cu–N–Cu* (deg)	Cu···Cu* (Å)	<i>J</i> (cm ⁻¹)	ref
[Cu ₂ (H ₂ L ₂)] [Cu ₂ (N ₃) ₆]	1.975(7)	1.982(7)	104.1(3)	3.121(2)	-42	25a
{[Cu ₂ (tppz)(N ₃) ₂][Cu ₂ (N ₃) ₆]} _n	1.980(2)	1.988(3)	102.93(10)	3.103(6)	+3.4	26
{K ₂ [Cu ₂ (N ₃) ₆][Cu(pyrazinato)(N ₃)]} _n	2.011(5)	1.997(6)	102.5(2)	3.126(2)		25b
[Bu ₄ N] ₂ [Cu ₂ (N ₃) ₆] 1	1.953(5)	2.006(4)	104.3(2)	3.126(2)	-36	this study

Accordingly, the data were fitted to an expression derived from a high-temperature series expansion for an $S = 1/2$ Heisenberg chain:²⁸

$$\chi'_M = \frac{Ng^2\beta^2(N)}{4kT(D)}^{2/3} \quad (1)$$

where $N = 1.0 + 5.797\,9916y + 16.902\,653y^2 + 29.376\,885y^3 + 29.832\,959y^4 + 14.036\,918y^5$, $D = 1.0 + 2.79799y + 7.008\,6780y^2 + 8.653\,8644y^3 + 4.574\,3114y^4$, and $y = J/2kT$.

The spin Hamiltonian formalism considered was $-J\sum S_i S_{i+1}$. The experimental molecular magnetic susceptibilities, χ_M , previously mentioned refer to 1 mol of [Pr₄N]₂[Cu₃(N₃)₈], and in contrast, eq 1 refers to 1 mol of $S = 1/2$ spins, which implies $\chi_M = 3\chi'_M$.

Fits were carried out down to 16 K, below which the theoretical curve and experimental data diverged. The best-fit parameters were $J = 7.0(4)$ cm⁻¹ and $g = 2.246$ with an agreement factor of $R = 7.5 \times 10^{-5}$. Figure 6 shows the results of this fit. The $\chi_M T$ decrease below 5.8 K may arise for different reasons. Weak antiferromagnetic interchain interactions, although unlikely because of the large distance (~10.5 Å) between chains which are separated by the bulky [Pr₄N]⁺ cations, cannot be discarded because of the numerous hydrogen contacts between anions and cations. For example, the nitrogen atoms of two terminal (N6, N18) and three bridging azido ligands (N9, N21, N24) are hydrogen bonded to carbon atoms of the [Pr₄N]⁺ cations. Zero-field splitting effects may also be responsible for this $\chi_M T$ decrease below 5.8 K but could not be taken into account within the context of the approach used. However, to illustrate the effects of Zeeman splitting under the influence of the applied magnetic field, magnetic susceptibility simulations were carried out with the MAGPACK program package²⁹ for a Cu₁₀ ring. Calculations according to the isotropic case (ISOMAG) predicted no $\chi_M T$ drop. However, the anisotropic case

(ANIMAG) predicted such a drop below 3 K for $J > 0$ and an applied field of 10 kG. Therefore, in agreement with previous reports,³⁰ we suggest that the origin of this $\chi_M T$ decrease at low temperature may rather be a Zeeman splitting of the $\pm m_S$ levels within the lowest-lying spin multiplets.

Concluding Remarks

Complexes **1** and **2** are the first examples of Cu^{II} compounds including exclusively azido ligands acting either as terminal donors or as $\mu_{1,1}$ -N_{azido} bridges. In complex **1**, although the Cu^{II}–N_{azido}–Cu^{II} angle is moderately large (104.3°), the intraduclear magnetic interaction is significantly antiferromagnetic ($J = -36(2)$ cm⁻¹). On the other hand, in complex **2**, the smaller Cu^{II}–N_{azido}–Cu^{II} angles (average values for Cu1–N_{azido}–Cu2, Cu2–N_{azido}–Cu3, and Cu1–N_{azido}–Cu3* are 99.35°, 99.28°, and 101.58°, respectively) allow for prevalence of the ferro- over the antiferromagnetic contribution to the magnetic interactions extended over the 1D chains. As a whole, these results not only confirm the prevailing role of the Cu^{II}– $\mu_{1,1}$ -N_{azido}–Cu^{II} angle on the ferro- vs the antiferromagnetic nature of the magnetic interaction in these doubly EO azido bridged Cu^{II} systems but also tend to validate the lower value recently predicted for the critical angle (~104°).⁷

Acknowledgment. The work was financially supported by the University Grants Commission, New Delhi, by a grant (F.12-9/2002(SR-I)) to S.K. Financial support from the Center for Nanoscience and Technology, Jadavpur University, is also gratefully acknowledged. We are grateful to the National X-ray Diffraction Facility, IIT Bombay, for collection of intensity data of complex **2** (on chargeable basis).

Supporting Information Available: Further details of structure determination, including tables of atomic coordinates, anisotropic displacement parameters, bond lengths, and bond angles for the complexes **1**, **2**, and **3**, and a magnetic susceptibility simulation plot of complex **2** using the MAGPACK program package²⁹ for a Cu₁₀ ring. This material is available free of charge via the Internet at <http://pubs.acs.org>.

IC050117U

(28) Baker, G. A., Jr.; Rushbrooke, G. S.; Gilbert, H. E. *Phys. Rev. A* **1964**, *135*, 1272.

(29) (a) Borrás-Almenar, J. J.; Clemente-Juan, J. M.; Coronado, E.; Tsukerblat, B. S. *Inorg. Chem.* **1999**, *38*, 6081. (b) Borrás-Almenar, J. J.; Clemente-Juan, J. M.; Coronado, E.; Tsukerblat, B. S. *J. Comput. Chem.* **2001**, *22*, 985.

(30) (a) Gutierrez, L.; Alzuet, G.; Real, J. A.; Cano, J.; Borrás, J.; Castiñeiras, A. *Inorg. Chem.* **2000**, *39*, 3608. (b) González-Álvarez, M.; Alzuet, G.; Borrás, J.; Macías, B.; Castiñeiras, A. *Inorg. Chem.* **2003**, *42*, 2992. (c) Glaser, T.; Heidemeier, M.; Grimme, S.; Bill, E. *Inorg. Chem.* **2004**, *43*, 5192.